

# Hydrothermal synthesis, structures, luminescence and magnetic properties of Zn(II) and Cu(II) complexes with new hydrazone ligand

Chang-zheng Zheng, Liang Wang\*, Juan Liu

School of Environmental and Chemical Engineering, Xi'an Polytechnic University, Xi'an 710048, PR China

## ARTICLE INFO

### Article history:

Received 3 July 2011

Received in revised form 2 October 2011

Accepted 7 November 2011

Available online 29 November 2011

### Keywords:

Hydrothermal synthesis

Hydrazone ligand

Complexes

Crystal structure

Luminescence

Magnetic properties

## ABSTRACT

Two new complexes  $[\text{Zn}(\text{HL})_2(\text{py})_2]$  (**1**) and  $[\text{Cu}(\text{HL})_2]$  (**2**) have been synthesised from a bidentate Schiff base ligand **HL** (benzylidene acetophenone benzoyl hydrazone). The crystal structures of complex **1** and complex **2** were determined by single-crystal X-ray diffraction. The data indicate that: the complex **1** crystallizes in the monoclinic space group  $P2(1)/n$ , with  $a$  (nm) = 1.35816(8),  $b$  (nm) = 2.39486(13),  $c$  (nm) = 1.41368(8),  $\alpha$  ( $^\circ$ ) = 90,  $\beta$  ( $^\circ$ ) = 96.0840(10),  $\gamma$  ( $^\circ$ ) = 90,  $Z$  = 4. The complex **2** crystallizes in the triclinic space group  $P-1$ , with  $a$  (nm) = 1.02483(8),  $b$  (nm) = 1.35797(11),  $c$  (nm) = 1.38271(11),  $\alpha$  ( $^\circ$ ) = 71.5020(10),  $\beta$  ( $^\circ$ ) = 78.5850(10),  $\gamma$  ( $^\circ$ ) = 74.3110(10),  $Z$  = 1. Moreover, the unsaturated coordination site of metal ion is occupied by secondary ligand of pyridine. The mononuclear units in **1** and **2** are packed through weak  $\text{C}-\text{H} \cdots \pi$  and  $\pi-\pi$  interactions respectively. The results of analytical, IR and TG analysis studies are presented in this paper. Both the ligand and complex **1** show fluorescence in DMF solutions at room temperature. The complex **2** variable-temperature (300–1.8 K) magnetic test show that there is ferromagnetic intramolecular interaction and weak antiferromagnetic intermolecular interaction.

© 2011 Elsevier B.V. All rights reserved.

## 1. Introduction

Metal–organic coordination compounds have raised an upsurge of interest in the fields of crystal engineering and functional materials, due to their intriguing structural features as well as desired properties [1–4]. The rational design and synthesis of novel coordination complexes based on transition or non-transition metals and multifunctional bridging ligands is of great research interest, due to their interesting topologies and potential applications as functional materials. Schiff bases are very interesting compounds because of their model character and practical applications [5,6] and also these are very important classes of organic compounds from both practical and theoretical points of view. Methods of synthesis and numerous applications in organic chemistry of compounds have been summarized [7]. In recent years, transition metal complexes of asymmetrical Schiff base ligands have attracted enormous attentions due to their diversity of molecular structures [8–12] and important properties, such as catalysis, porosity, chirality, luminescence, non-linear optics, ferroelectrics, magnetism [13–21]. Hydrazone is not only an important compound of Schiff bases but also a major polydentate ligands. Due to their variable bonding when forming complexes with metal ions, the coordination chemistry of hydrazones has been intensively investigated. In terms of chemical field hydrazones have

been attracting much attention because of their chemical and industrial versatility, and strong tendency to chelate to transition metals [22,23], lanthanide metals [24] and main group metals [25,26].

To the best of our knowledge, the chemical properties of complexes can be tuned to force metal ions to adopt unusual coordination geometry. The present work is a part of our study on the metal complexes of benzoyl hydrazone. Herein we report the synthesis, structure, fluorescence and magnetic properties of the compounds,  $\text{C}_{54}\text{H}_{44}\text{N}_6\text{O}_2\text{Zn}$  and  $\text{C}_{88}\text{H}_{68}\text{N}_8\text{O}_4\text{Cu}_2$ . The procedure of synthesis (**HL**) is shown in Scheme 1.

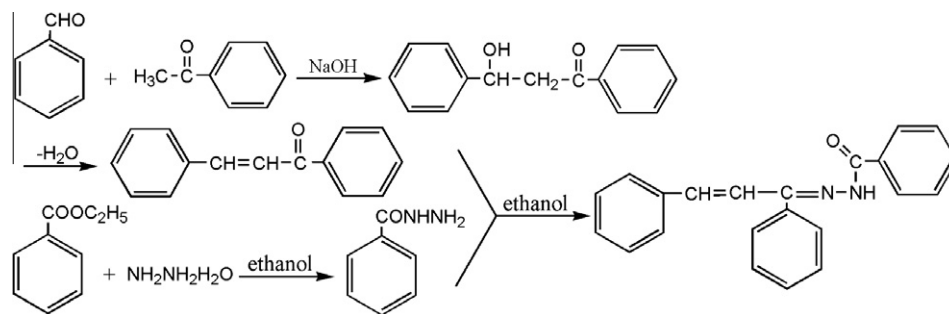
## 2. Experimental

### 2.1. Materials and measurements

All starting materials and solvents used in this work were of analytical grade and used as purchased from Sinopharm Chemical Reagent Co. Ltd. without further purification. Elemental analyses (C, H, N) were performed using a Vario EL elemental analyzer. FT-IR spectrum was measured as KBr pellets on a Nicolet Nexus FT-IR spectrometer in the 4000–400  $\text{cm}^{-1}$  region. Thermogravimetric analyses (TGA) were carried out on a Perkin–Elmer Pyris-1, Thermogravimetric analyzer operating at a heating rate of 10  $\text{K min}^{-1}$  in a flow of dry oxygen-free nitrogen at 20  $\text{mL min}^{-1}$ . Fluorescence measurements were performed on a Model RF-5 spectrofluorimeter. The temperature dependence magnetic susceptibilities were measured

\* Corresponding author. Tel.: +86 29 82330169.

E-mail address: [wllily315668256@yahoo.com.cn](mailto:wllily315668256@yahoo.com.cn) (L. Wang).



Scheme 1. Synthetic route of the ligand.

on polycrystalline samples with a Quantum Design SQUID MPMS-XL susceptometer operating at a magnetic field 0.1 T over a temperature range 1.8–300 K. The crystal structures were determined by single-crystal X-ray diffraction. SHELXS97, SHELXL97 software were then used for structure solution and refinement correspondingly.

## 2.2. Preparation of the ligand

Acetophenone (3.00 g, 0.025 mol), benzaldehyde (2.66 g, 0.025 mol) and sodium hydroxide (12.5 mL, concentration: 10%) were mixed in 7.50 mL ethanol at room temperature and the mixture was refluxed for 7 h stirringly. Then the crystals were precipitated and collected by filtration. Finally the product was recrystallized from ethanol and dried under reduced pressure to give compound of benzylidene acetophenone. Yield: 76%. The schematic diagram showing the synthesis of it is shown in Scheme 1. Anal. Calcd. (%) for  $C_{15}H_{12}O$ : C, 86.42; H, 5.76; N, 0. Found (%): C, 86.50; H, 5.81; N, 0. Selected IR (KBr pellet,  $cm^{-1}$ ):  $\nu(C=C)$  1598, 1503;  $\nu(C=O)$  1741;  $\nu(C=N)$  1650.

Ethyl benzoate (3.76 g, 0.025 mol) was dissolved in anhydrous ethanol (20 mL) at room temperature and heated at 363 K. Hydrazine hydrate (1.50 g, 0.030 mol) was added into the mixture. After being refluxing for 7–8 h, the mixture was cooled to room temperature. Then the crystals were precipitated and collected by filtration. Finally, the product was recrystallized from ethanol and dried under reduced pressure to give compound of benzoyl hydrazine. Yield: 72% (synthetic route is described as Scheme 1). Anal. Calcd. (%) for  $C_7H_8N_2O$ : C, 61.71; H, 5.84; N, 20.51. Found (%): C, 61.75; H, 5.92; N, 20.58. Selected IR (KBr pellet,  $cm^{-1}$ ):  $\nu(C=C)$  1592, 1522;  $\nu(C=O)$  1735;  $\nu(N-H)$  3253;  $\nu(C-N)$  1205.

Benzoyl hydrazine (3.13 g, 0.023 mol) was dissolved in anhydrous ethanol (30 mL) at room temperature and heated at 373 K. Benzylidene acetophenone (4.79 g, 0.023 mol) was added into the mixture. After being refluxing for 7–8 h, the mixture was cooled to room temperature. Then the crystals were precipitated and collected by filtration. Finally, the product was recrystallized from ethanol and dried under reduced pressure to give compound benzylidene acetophenone benzoyl hydrazone (HL). Yield: 65% (synthetic route is described as Scheme 1). Anal. Calcd. (%) for  $C_{22}H_{18}N_2O$ : C, 80.86; H, 5.52; N, 8.52. Found (%): C, 80.98; H, 5.56; N, 8.59. Selected IR (KBr pellet,  $cm^{-1}$ ):  $\nu(C=C)$  1602;  $\nu(C=O)$  1682;  $\nu(C=N)$  1628;  $\nu(C-N)$  1215.

## 2.3. Preparation of the complex $[Zn(HL)_2(py)_2]$ (1)

A mixture of HL (0.0326 g, 0.10 mmol),  $Zn(NO_3)_2 \cdot 6H_2O$  (0.0297 g, 0.10 mmol), pyridine (0.0079 g, 0.10 mmol) and  $H_2O$  (5.00 mL), several drops of methanol were placed in a Parr Teflon-lined stainless steel vessel (25 mL), and then the vessel was sealed and heated at 413 K for 3 d. After the mixture was slowly cooled to room temperature, several colorless crystals were

obtained. Anal. Calcd. (%) for  $C_{54}H_{44}N_6O_2Zn$ : C, 74.22; H, 5.13; N, 9.67. Found (%): C, 74.18; H, 5.07; N, 9.61. Selected IR (KBr pellet,  $cm^{-1}$ ):  $\nu(C=C)$  1545;  $\nu(C-N)$  1209;  $\nu(N-H)$  3244;  $\nu(C-O)$  1276.

## 2.4. Preparation of the complex $[Cu(HL)]_2$ (2)

A mixture of HL (0.0326 g, 0.10 mmol),  $Cu(NO_3)_2 \cdot 3H_2O$  (0.0242 g, 0.10 mmol) and  $H_2O$  (5.00 mL), several drops of methanol solution were placed in a Parr Teflon-lined stainless steel vessel (25 mL), and then the vessel was sealed and heated at 413 K for 3 d. After the mixture was slowly cooled to room temperature, several blue crystals were obtained. Anal. Calcd. (%) for  $C_{88}H_{68}N_8O_4Cu_2$ : C, 74.02; H, 4.83; N, 7.81. Found (%): C, 73.98; H, 4.80; N, 7.85. Selected IR (KBr pellet,  $cm^{-1}$ ):  $\nu(C=C)$  1551;  $\nu(C-N)$  1213;  $\nu(N-H)$  3241;  $\nu(C-O)$  1268.

## 2.5. X-ray crystal structure determinations

Diffraction intensities for two complexes were collected on a Bruker SMART 1000 CCD area-detector with Mo K $\alpha$  radiation ( $\lambda = 0.71073 \text{ \AA}$ ) using an  $\omega$  scan mode at  $298 \pm 2 \text{ K}$  (complexes 1 and 2). Diffraction intensity data were collected in the  $\theta$  range of 1.73–25.05 for complex 1 and 1.62–25.05 for complex 2. The collected data were reduced using the SAINT program [27], and empirical absorption corrections were performed using the SADABS program [28]. Two structures were solved by direct methods and refined using full-matrix least square techniques on  $F^2$  with

Table 1  
Crystal data and structure refinement for complexes 1–2.

	1	2
Formula	$C_{54}H_{44}N_6O_2Zn$	$C_{88}H_{68}N_8O_4Cu_2$
Fw	874.32	1428.66
T (K)	298(2)	298(2)
Cryst. syst.	Monoclinic	Triclinic
Space group	$P2(1)/n$	$P-1$
a ( $\text{\AA}$ )	13.5816(8)	10.2483(8)
b ( $\text{\AA}$ )	23.9486(13)	13.5797(11)
c ( $\text{\AA}$ )	14.1368(8)	13.8271(11)
$\alpha$ ( $^\circ$ )	90	71.5020(10)
$\beta$ ( $^\circ$ )	96.0840(10)	78.5850(10)
$\gamma$ ( $^\circ$ )	90	74.3110(10)
V ( $\text{\AA}^3$ )	4572.2(4)	1743.6(2)
Z	4	1
$\rho$ calcd. ( $\text{mg m}^{-3}$ )	1.270	1.361
F(000)	1824	742
$\theta$ rang. ( $^\circ$ )	1.73–25.05	1.62–25.05
$\mu$ ( $\text{mm}^{-1}$ )	0.585	0.671
$\lambda$ ( $\text{\AA}$ )	0.71073	0.71073
R (int)	0.0304	0.0200
$R_1, wR_2 [I > 2\sigma(I)]$	0.0480, 0.1391	0.0407, 0.0899
$R_1, wR_2$ (all data)	0.0755, 0.1632	0.0579, 0.0968
Peak and hole ( $e\text{\AA}^{-3}$ )	0.725, -0.564	0.220, -0.273

**Table 2**  
Selected bond distances (Å) and bond angles (°) for complexes **1–2**.

Distances	Å	Angle	°	Angle	°
<b>1</b>					
Zn(1)–O(1)	2.065(2)	O(1)–Zn(1)–O(2)	175.24(9)	O(2)–Zn(1)–N(4)	74.56(10)
Zn(1)–O(2)	2.075(2)	O(1)–Zn(1)–N(5)	86.89(10)	N(5)–Zn(1)–N(4)	89.54(11)
Zn(1)–N(5)	2.166(3)	O(2)–Zn(1)–N(5)	88.44(10)	N(2)–Zn(1)–N(4)	93.64(10)
Zn(1)–N(2)	2.173(3)	O(1)–Zn(1)–N(2)	75.46(10)	O(1)–Zn(1)–N(6)	87.95(11)
Zn(1)–N(4)	2.220(3)	O(2)–Zn(1)–N(2)	109.23(10)	O(2)–Zn(1)–N(6)	91.58(10)
Zn(1)–N(6)	2.231(3)	N(5)–Zn(1)–N(2)	162.26(12)	N(2)–Zn(1)–N(6)	86.03(11)
<b>2</b>					
Cu(1)–O(1)	1.8902(15)	O(1)–Cu(1)–O(2)	177.79(7)	O(2)–Cu(1)–N(2)	101.16(7)
Cu(1)–O(2)	1.9278(15)	O(1)–Cu(1)–N(4)	97.61(7)	N(4)–Cu(1)–N(2)	165.30(8)
Cu(1)–N(4)	2.025(2)	O(2)–Cu(1)–N(4)	80.36(7)	C(7)–O(1)–Cu(1)	112.37(14)
Cu(1)–N(2)	2.0373(19)	O(1)–Cu(1)–N(2)	80.58(7)	N(1)–N(2)–Cu(1)	110.53(13)

**Table 3**  
C–H... $\pi$  parameters donor/acceptor scheme (Å, °) for **1**.

D–H...A	D–H	H...A	D...A	D–H...A
C47–H47...Cg1	0.931	2.197	3.076	128.284
C46–H46...Cg2	0.931	2.687	3.495	151.747

the program SHELXL-97 [29]. All non-hydrogen atomic positions were located in difference Fourier maps and refined anisotropically. Some of hydrogen atoms were placed in their geometrically generated positions and other hydrogen atoms were located from the different Fourier map and refined isotropically. Crystallographic data are given in Table 1. Selected bond distances and angles are given in Table 2. C–H... $\pi$  parameters donor/acceptor scheme (Å, °) for **1** are given in Table 3.

### 3. Results and discussion

#### 3.1. Structure descriptions of the complex **1**

As shown in Fig. 1, there is one independent molecule in the asymmetric unit. Complex **1** is mononuclear six-coordinated zinc. The coordination environment of Zn is comprised of two pyridine ligands and two hydrazone ligands (two O atoms, four N atoms). The zinc(II) center in **1** adopts a similar to distorted octahedron configuration (Fig. 2). O1, N2, O2 and N5 constitute a pyramid's bottom. N4 and N6 occupy the top position, which complete the coordination environment of Zn center. The bond lengths of Zn(1)–N(2), Zn(1)–N(4), Zn(1)–N(5) and Zn(1)–N(6) are 2.173(3) Å, 2.220(3) Å, 2.166(3) Å and 2.231(3) Å, respectively, these data indicate the bonds are very close to the complex with identical coordination [30]. The Zn(1)–O(1), Zn(1)–O(2) bond

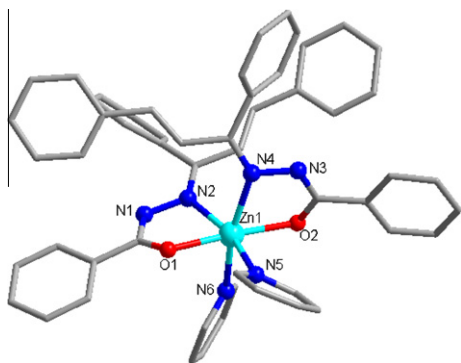


**Fig. 1.** Molecular structure of the title complex **1**.

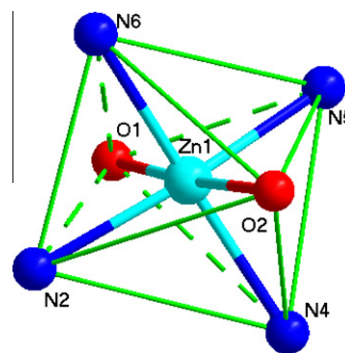


**Fig. 2.** Coordinated circumstance of Zn(II).

distances are 2.065(2) Å and 2.075(2) Å, respectively, which are shorter than reported [30]. C(7)–N(1) (1.318(4) Å), C(29)–N(3) (1.313(4) Å) and C(30)–N(4) (1.304(4) Å) are longer than the C=N double bond (1.30 Å), but shorter than the C–N single bond (1.443 Å). Different angles around the zinc atom and their sum of 360.02° indicate a nearly coplanar geometry of the metal environment. The N(4)–Zn(1)–N(6) angle is 165.23°, which indicates that N(4) and N(6) are closely located at the vertical line of the plane. The bonds of [C(7)–O(1) (1.278(4) Å), C(29)–O(2) (1.287(4) Å), C(7)–N(1) (1.318(4) Å), C(29)–N(3) (1.313(4) Å)] are compared with [C–O (1.43 Å), C=O (1.20 Å), C–N (1.47 Å), C=N (1.27 Å)] suggesting an enol coordination model for ligands. Bond lengths of C(6)–C(7) (1.494(5) Å) and C(8)–C(15) (1.453(5) Å) confirm the sp<sup>2</sup> hybridization of carbon atom [31]. The mononuclear units in **1** are packed alongside with each other through weak C–H... $\pi$  interactions. Along with this shortest interaction (H47 to the centroid of ring C1–C6: 2.197 Å) propagating crystallographic *c*-axis, another relatively weak C–H... $\pi$  interaction (H46 to the centroid of ring C9–C14: 2.687 Å) runs in the direction of *c*-axis with the formation of a 2D sheet structure (Fig. 3). For **1**, Cg1 phenyl ring C1–C6 at *x*, *y*, *z*; Cg2 phenyl ring C9–C14 at  $-0.5 + x$ ,  $0.5 - y$ ,  $-0.5 + z$ .

#### 3.2. Structure descriptions of the complex **2**

The structure of compound **2** is shown in Fig. 4, accompanied by an atomic numbering scheme for the asymmetric unit. Complex **2** is dinuclear five-coordinated copper. The coordination environment of Cu is comprised of two hydrazone ligands (three O atoms, two N atoms). The copper(II) center in **2** adopts a structure which is similar to double-pyramid configuration (Fig. 5). O1, N2, O2 and N4 constitute a pyramid's bottom. O2A occupies the top position, which complete the coordination environment of Cu center

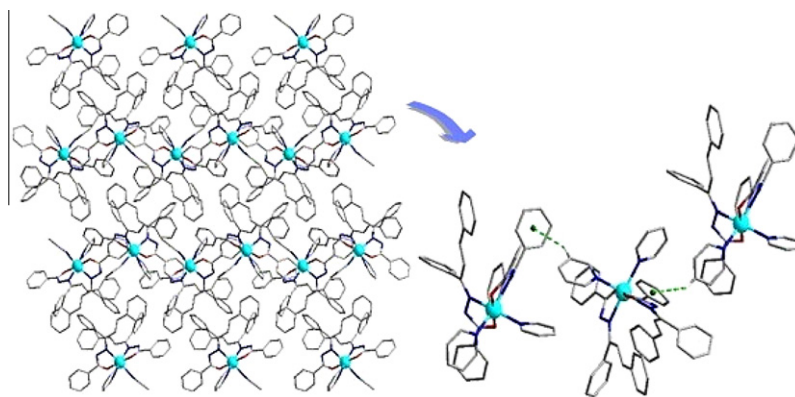


Fig. 3. A view of 2D sheet structure in **1** formed through C–H... $\pi$  interactions.

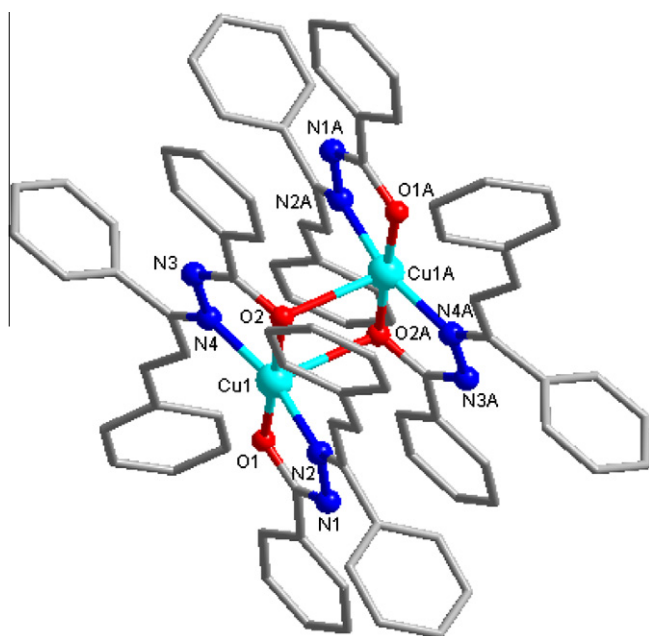


Fig. 4. Molecular structure of the title complex **2**.

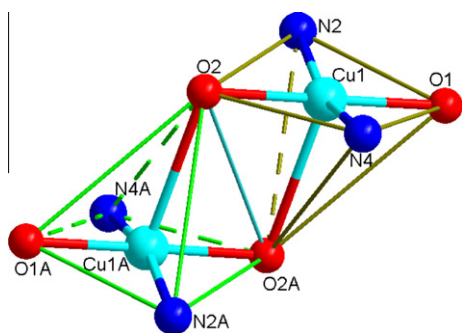


Fig. 5. Coordinated circumstance of Cu(II).

(symmetry code:  $[1-x, 1-y, 1-z]$ ). The bond lengths of Cu(1)–N(2) and Cu(1)–N(4) are 2.037(19) Å and 2.025(2) Å. These are very close to the complex with identical coordination [32]. The Cu(1)–O(1), Cu(1)–O(2) bond distances are 1.890(15) Å and 1.928(15) Å, respectively, which are shorter than the reported

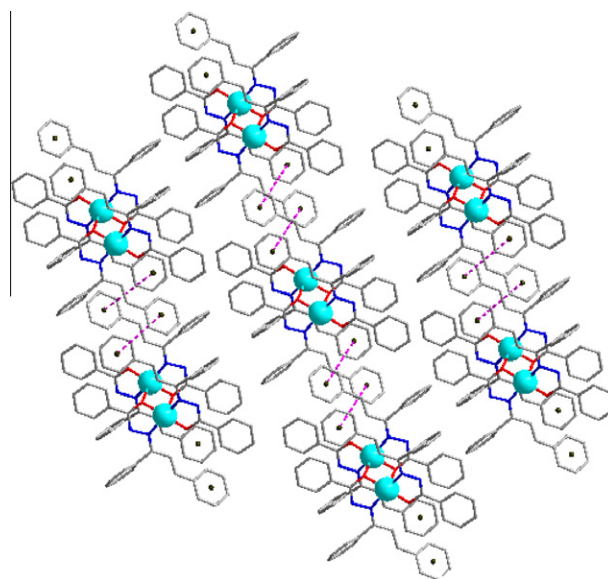


Fig. 6. A view of 2D sheet structure in **2** formed through  $\pi$ – $\pi$  interactions.

[33]. C(7)–N(1) (1.309(3) Å) and C(8)–N(2) (1.317(3) Å) are longer than the C=N double bond (1.30 Å) but shorter than the C–N single bond (1.443 Å). Different angles around the copper atom and their sum of  $359.71^\circ$  indicate a nearly coplanar geometry of the metal environment. The bonds of [C(7)–O(1) (1.292(3) Å), C(29)–O(2) (1.308(3) Å), C(7)–N(1) (1.309(3) Å), C(29)–N(3) (1.301(3) Å)] are compared with [C–O (1.43 Å), C=O (1.20 Å), C–N (1.47 Å), C=N (1.27 Å)] suggesting an enol coordination model for ligands. Bond lengths of C(6)–C(7) (1.476(3) Å) and C(8)–C(15) (1.443(3) Å) confirm the  $sp^2$  hybridization of carbon atom [31]. The dinuclear units in **2** are packed alongside with each other through weak  $\pi$ – $\pi$  interactions. There are  $\pi$ – $\pi$  interactions between the aromatic rings of the neighboring chain with a centroid–centroid distance between neighboring aromatic rings of 3.3624(4) Å, generating an extended two-dimensional architecture (Fig. 6). For **2**, Cg1 phenyl ring C17–C22 at  $1-x, 1-y, -z$ ; Cg2 phenyl ring C39–C44 at  $1-x, 1-y, 1-z$ .

### 3.3. Thermogravimetric analysis

Thermogravimetric analysis (TGA) was carried out to examine the thermal stability of the two compounds. The crushed single-crystal sample was heated up to 1000 °C in  $N_2$  at a heating rate

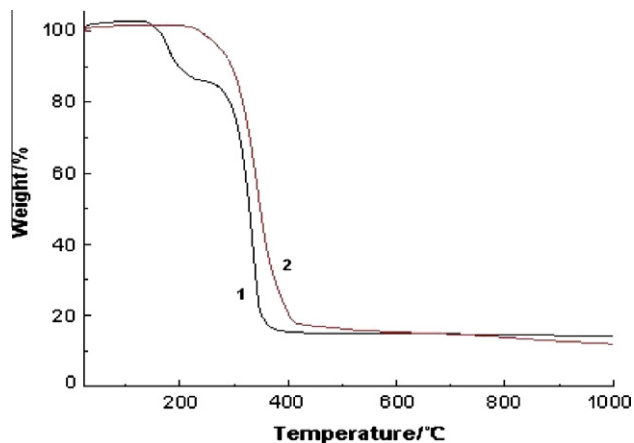


Fig. 7. TG curves of compounds **1** and **2**.

of  $10\text{ }^{\circ}\text{C min}^{-1}$ . The typical TG curves of the two compounds are shown in Fig. 7, respectively.

The TG curves for **1** show that it is stable up to  $158.39\text{ }^{\circ}\text{C}$  without any weight loss, which means the compound could retain structural integrity to  $158.39\text{ }^{\circ}\text{C}$ . From  $158.39$  to  $191.68\text{ }^{\circ}\text{C}$ , the total loss of  $16.95\%$  is consistent with the pyrolysis of pyridyl fragments. From  $296.79$  to  $334.10\text{ }^{\circ}\text{C}$ , the total loss of  $70.48\%$  is consistent with the pyrolysis of coordinated benzoyl hydrazine fragments and benzene-methyl phenylethyl fragments. The final residue was probably ZnO (remaining weight: found:  $9.26\%$ , calcd.  $12.57\%$ ).

The TG curves for **2** show that it is stable up to  $291.05\text{ }^{\circ}\text{C}$  without any weight loss, which means the compound could retain structural integrity to  $291.05\text{ }^{\circ}\text{C}$ . From  $291.05$  to  $363.05\text{ }^{\circ}\text{C}$ , the total loss of  $84.39\%$  is consistent with the pyrolysis of benzene-methyl phenylethyl fragments and hydrazine groups fragments. The final residue was probably CuO (remaining weight: found:  $11.19\%$ , calcd.  $15.61\%$ ).

### 3.4. Luminescence behaviors

The photoluminescence behavior of the free Schiff base ligand (**HL**) and its corresponding zinc(II) compounds were studied in the solid state at room temperature. The emission spectra of **HL** and compound **1** are depicted in Fig. 8. Upon photoexcitation at  $402\text{ nm}$ , the free **HL** exhibits a broad fluorescent emission centered at  $409\text{ nm}$  and  $436\text{ nm}$ . Upon photoexcitation at  $452\text{ nm}$ , the corresponding compound **1** show more intense photoluminescence with the main emission at  $463\text{ nm}$ . The emission band for compound **1** is different to that found for the free ligand in terms of position and band shape. Therefore, the luminescence behaviors [34–36] in **1** may be attributed to the intraligand  ${}^1(\pi-\pi^*)$  transition, and greater intensity may presumably be due to the increase in conformational rigidity of the ligand upon coordination. Meanwhile, compared with the emission spectrum of **HL**, a apparently red shift of  $54\text{ nm}$  in **1** has been observed, which is considered to mainly arise from the coordination effect of Zn(II) with the ligand. Furthermore, the incorporation of Zn(II) effectively increases the conformational rigidity of **HL** and reduces the loss of energy via vibration motions. Thus, the enhanced fluorescence intensities of the two compounds are detected.

### 3.5. Magnetic properties

Variable temperature magnetic susceptibility  $\chi_M$  measurements (in the range of  $1.8\text{--}300\text{ K}$ ) for complex **2** were carried out

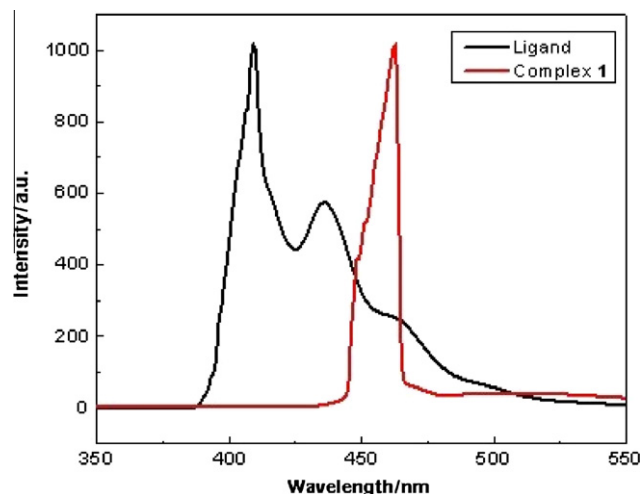


Fig. 8. Emission spectra: fluorescence in DMF solutions at  $298\text{ K}$  of ligand and complex **1**.

with a Quantum Design (SQUID) magnetometer MPMS-XL-5 in a field of  $1000\text{ Oe}$  (Fig. 9) on a powdered fresh sample from the same uniform batch. Moreover, we use a dinuclear copper model with  $\hat{H} = -2J\hat{S}_1\hat{S}_2$  ( $S_1 = S_2 = 1/2$ ) given by the equation as follows:

$$\chi_M = \frac{2Ng^2\beta^2}{K(T-\theta)} \left[ \frac{5 + \exp(-4J/KT)}{5 + 3\exp(-4J/KT) + \exp(-6J/KT)} \right]$$

to simulate the experimental results of  $\chi_M T$  vs.  $T$  and  $\chi_M$  vs.  $T$  plots [37].  $\chi_M$  is the dinuclear copper complexes molecular moore susceptibility;  $\theta$  is the Curie–Weiss parameters;  $N$  is the Avogadro's constant;  $g$  is the Landé factor;  $K$  is the Boltzmann constant;  $\beta$  is the Bohr magneton;  $T$  is the temperature;  $J$  is the dinuclear copper units of magnetic interaction parameters.

As can be seen from Fig. 9, the complex **2** with  $\chi_M$  value of lower temperature and increase gradually, in  $12\text{ K}$ ,  $\chi_M$  value began near a sharp increase. As can be seen from the plots of experimental data, the experimental  $\chi_M T$  value at  $300\text{ K}$  is  $1.17\text{ emu K mol}^{-1}$ . These values are the expected ones for two magnetically quasi-isolated spin doublets. Upon cooling down, the  $\chi_M T$  value continuously increases, reaching a maximum value of  $1.27\text{ emu K mol}^{-1}$  at  $50\text{ K}$ . This behavior of the  $\chi_M T$  curve shows that there exist ferromagnetic interactions in complex **2**. As the temperature further reduced,  $\chi_M T$  value has decreased, indicating a weaker

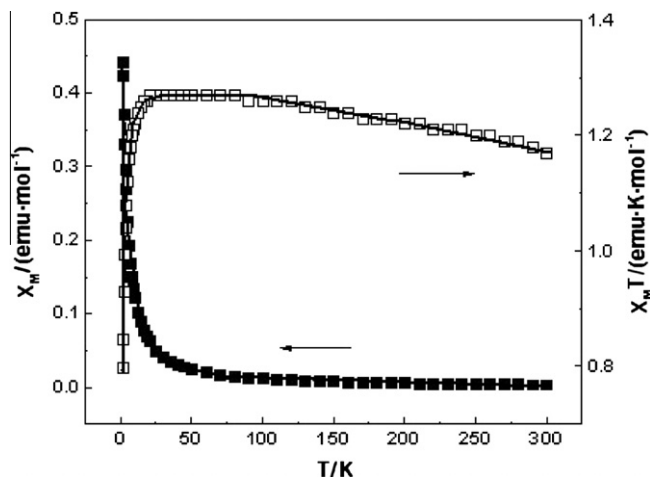


Fig. 9. Temperature dependence of  $\chi_M$  and  $\chi_M T$  vs.  $T$  for complex **2**.

molecular antiferromagnetic coupling effect. A best fit leads to the following values:  $g = 2.16$ ,  $\theta = -0.8$  K and  $J = -12.8$  cm<sup>-1</sup>. In conclusion, magnetic results show that there is a ferromagnetic intramolecular interaction and weak antiferromagnetic intermolecular interaction in the complex **2**.

#### 4. Conclusions

Its transition metal complexes ([Zn(HL)<sub>2</sub>(py)<sub>2</sub>], [Cu(HL)<sub>2</sub>]) are obtained successfully using an asymmetrical ligand with Schiff base has been designed and synthesised in this work. The studies of their crystal structures and supramolecular interactions indicate that the diversity of structural motifs. Systematic characterizations of the two complexes by elemental analysis, FT-IR and TG analysis studies have also been discussed. Complex **1** is mononuclear six-coordinated zinc. The zinc(II) center in **1** adopts a similar to distorted octahedron configuration. Complex **2** is dinuclear five-coordinated copper. The copper(II) center in **2** adopts a structure which is similar to double-pyramid configuration. The free HL exhibits a broad fluorescent emission centered at 409 nm and 436 nm. It is found that the corresponding zinc(II) compound **1** show more intense photoluminescence with the main emission at 463 nm. The luminescence behaviors in **1** may be attributed to the intraligand <sup>1</sup>( $\pi$ - $\pi^*$ ) transition, and greater intensity may presumably be due to the increase in conformational rigidity of the ligand upon coordination. There is a ferromagnetic intramolecular interaction and weak antiferromagnetic intermolecular interaction in complex **2**.

#### Supplementary material

Crystallographic data (excluding structure factors) for the structure(s) reported in this paper have been deposited with the Cambridge Crystallographic Data Centre as supplementary publication numbers: CCDC\_827557 (**1**), CCDC\_827558 (**2**). These data can be obtained free of charge from the Cambridge Crystallographic Data Centre (CCDC), CCDC, 12, Union Road, Cambridge CB2 1EZ, UK; fax: +44 1223 336 033; E-mail: deposit@ccdc.cam.ac.uk.

#### Acknowledgment

We thank the Natural Science Foundation of Shaanxi Province, People's Republic of China (2009JM2012) for financial support.

#### References

- [1] C.V.K. Sharma, *Cryst. Growth Des.* 2 (2002) 465.
- [2] J.-P. Zhang, X.-M. Chen, *Chem. Commun.* (2006) 1689.
- [3] B. Kesanli, W.-B. Lin, *Coord. Chem. Rev.* 246 (2003) 305.
- [4] R.E. Morris, P.S. Wheatley, *Angew. Chem. Int. Ed. Engl.* 47 (2008) 4966.
- [5] H. Hadjoudis, *Mol. Eng.* 5 (1995) 301.
- [6] T. Dziembowska, *Pol. J. Chem.* 72 (1998) 193.
- [7] K. Wozniak, E. Grech, A. Szady-Chelminiecka, *Pol. J. Chem.* 74 (2000) 717.
- [8] Z.-L. You, Q.-Z. Jiao, S.-Y. Niu, J.-Y. Chi, *Z. Anorg. Allg. Chem.* 632 (2006) 2486.
- [9] Y. Harada, G.S. Girolami, *Polyhedron* 26 (2007) 1758.
- [10] W.-X. Ni, M. Li, X.-P. Zhou, Z. Li, X.-C. Huang, D. Li, *Chem. Commun.* (2007) 3479.
- [11] W. Plass, H.P. Yozgatli, *Z. Anorg. Allg. Chem.* 629 (2003) 65.
- [12] E. Colacio, M. Ghazi, R. Kivekas, M. Klinga, F. Lloret, J.M. Moreno, *Inorg. Chem.* 39 (2000) 2770.
- [13] S. Thakurta, P. Roy, R.J. Butcher, M.S. El Fallah, J. Tercero, E. Garrriba, S. Mitra, *Eur. J. Inorg. Chem.* (2009) 4385.
- [14] S. Nayak, P. Gamez, B. Kozlevcar, A. Pevce, O. Roubeau, S. Dhenen, J. Reedijk, *Polyhedron* 29 (2010) 2291.
- [15] R.-Q. Zou, H. Sakurai, S. Han, R.-Q. Zhong, Q. Xu, *J. Am. Chem. Soc.* 129 (2007) 8402.
- [16] Y. Sunatsuki, Y. Motoda, N. Matsumoto, *Coord. Chem. Rev.* 226 (2002) 199.
- [17] C. Wallenhorst, G. Kehr, H. Luftmann, R. Frohlich, G. Erker, *Organometallics* 27 (2008) 6547.
- [18] S.K. Ghosh, S. Bureekaew, S. Kitagawa, *Angew. Chem. Int. Ed. Engl.* 47 (2008) 3403.
- [19] C. Sousa, P. Gameiro, C. Freire, B. de Castro, *Polyhedron* 23 (2004) 1401.
- [20] L.-F. Ma, Y.-Y. Wang, L.-Y. Wang, D.-H. Lu, S.R. Batten, J.-G. Wang, *Cryst. Growth Des.* 9 (2009) 2036.
- [21] H. Arora, F. Lloret, R. Mukherjee, *Inorg. Chem.* 48 (2009) 1158.
- [22] P. Cheng, D.-Z. Liao, S.-P. Yan, Z.-H. Jiang, G.-L. Wang, X.-K. Yao, H.-G. Wang, *Inorg. Chim. Acta* 248 (1996) 135.
- [23] H. Sur, *Acta Crystallogr.* C49 (1993) 870.
- [24] Y.-X. Ma, Z.-Q. Ma, G. Zhao, Y. Ma, M. Yang, *Polyhedron* 8 (1989) 2105.
- [25] S.-X. Liu, S. Gao, *Polyhedron* 17 (1998) 81.
- [26] S. Gao, Z.-Q. Weng, S.-X. Liu, *Polyhedron* 7 (1998) 3595.
- [27] SAINT Plus, Data Reduction and Correction Program, v. 6.01, Bruker AXS, Madison, Wisconsin, USA, 1998.
- [28] SADABS v.2.01, Bruker/Siemens Area Detector Absorption Correction Program, Bruker AXS, Madison, Wisconsin, USA, 1998.
- [29] G.M. Sheldrick, *Acta Cryst.* A64 (2008) 112.
- [30] Y.-M. Jiang, J.-M. Li, F.-Q. Xie, Y.-F. Wang, *Chin. J. Struct. Chem.* 25 (2006) 767.
- [31] G. Wojciechowski, M. Ratajczak-Sitarz, A. Katrusiak, W. Schilf, P. Przybylski, B. Brzezinski, *J. Mol. Struct.* 650 (2003) 191.
- [32] V.M. Nikitina, O.V. Nesterova, V.N. Kokozay, V.V. Dyakonenko, O.V. Shishkin, *J. Jeziarska, Inorg. Chem. Commun.* 12 (2009) 101.
- [33] Z.-L. You, L. Zhang, D.-H. Shi, X.-L. Wang, X.-F. Li, Y.-P. Ma, *Inorg. Chem. Commun.* 13 (2010) 996.
- [34] B. Dutta, P. Bag, U. Florke, K. Nag, *Inorg. Chem.* 44 (2005) 147.
- [35] S. Banthia, A. Samanta, *J. Phys. Chem. B* 110 (2006) 6437.
- [36] W. Chen, Q. Peng, Y. Li, *Cryst. Growth Des.* 8 (2008) 564.
- [37] O. Kahn, *Mol. Magnet.* (1993).